Pharmaceutical Sciences and Drug Design
ISSN: 3062-4428
2022, Volume 2, Page No: 193-211

Available online at: www.galaxypub.co/page/journals

Galaxy Publication

Piperine-Rich Baolier Capsule Promotes Cholesterol Excretion and Attenuates Atherosclerosis via LXRα Activation and Upregulation of ABCA1, ABCG5/8, and CYP7A1

Avery Cole[1]*, Nathan Reed[1], Mia Sanders[1]

[1]Department of Biotechnology, Faculty of Science, University of Sydney, Sydney, Australia.

***E-mail** ✉ avery.cole.au@gmail.com

Received: 16 August 2022; **Revised:** 21 November 2022; **Accepted:** 25 November 2022

ABSTRACT

Baolier capsule (BLEC), a traditional Mongolian formulation, is prescribed for managing hypercholesterolemia and atherosclerosis (AS). Yet, its therapeutic efficacy, key constituents, and molecular actions in these disorders remain insufficiently defined. This work sought to clarify the pharmacodynamic profile of BLEC, identify its principal bioactive molecules, and delineate its mechanisms against hypercholesterolemia and AS. Liver-specific LXRα knockout ApoE−/− mice were generated via adeno-associated virus injection through the tail vein. ApoE−/− mice were fed a high-fat diet to establish hyperlipidemia and AS models. Oil Red O staining of the aorta or liver was applied to evaluate the influence of oral BLEC, piperine, statins, or ezetimibe on plaque formation or hepatic lipid accumulation according to the study design. Serum lipid panels and cholesterol efflux markers were assessed using biochemical tests. Transcriptome analyses were used to determine BLEC-induced transcriptional alterations in the liver. HPLC-MS/MS quantified BLEC and its major constituents in hepatic tissue. Western blotting and qRT-PCR were employed to measure LXRα, ABCA1, ABCG5, ABCG8, and CYP7A1 expression. BLEC lowered lipid accumulation in both serum and hepatic tissue and mitigated AS by enhancing cholesterol disposal. BLEC and piperine, the dominant compounds identified in liver samples, stimulated LXRα, thereby elevating ABCA1, ABCG5, ABCG8, and CYP7A1 expression, which in turn facilitated cholesterol transfer to HDL and its removal through bile and feces. In addition, piperine showed cooperative beneficial effects when combined with atorvastatin or ezetimibe, two standard lipid-lowering medications. BLEC and its primary active constituent, piperine, boost cholesterol elimination, reduce circulating cholesterol, suppress AS progression, and demonstrate strong potential for clinical translation.

Keywords: Baolier Capsule, Atherosclerosis, Hypercholesterolemia, Cholesterol removal, Piperine, LC-MS/MS

How to Cite This Article: Cole A, Reed N, Sanders M. Piperine-Rich Baolier Capsule Promotes Cholesterol Excretion and Attenuates Atherosclerosis via LXRα Activation and Upregulation of ABCA1, ABCG5/8, and CYP7A1. Pharm Sci Drug Des. 2022;2:193-211. https://doi.org/10.51847/nbnvo1RuIC

Introduction

Atherosclerotic cardiovascular disease (ASCVD) remains a major global health challenge, representing the foremost cause of death worldwide and creating substantial medical and economic strain [1]. Evidence indicates that elevated cholesterol drives ASCVD, and lowering low-density lipoprotein cholesterol (LDL-C) reduces major cardiovascular event risk [2-4]. Clinically, LDL-C reduction is achieved mainly by blocking intestinal cholesterol uptake (ezetimibe), enhancing hepatic clearance of lipoproteins (Proprotein Convertase Subtilisin/Kexin Type 9 [PCSK9] inhibitors), and suppressing endogenous cholesterol production (statins) [5-7]. Although these therapies are widely used, many patients continue to experience recurrent cardiovascular disease, and their LDL-C levels often remain above guideline-recommended targets [8]. Crucially, current cholesterol-lowering agents do not function by directly accelerating cholesterol catabolism or excretion.

The ATP-binding cassette subfamily G proteins 5/8 (ABCG5/8) form a heterodimer responsible for transporting cholesterol into the bile and intestinal lumen [9]. Pharmacological activation of LXRα augments cholesterol efflux

by increasing ABCG5/G8 expression [10]. However, LXRα also upregulates Sterol Regulatory Element-Binding Protein 1 (SREBP1), which drives fatty acid synthesis, leading to unwanted hepatic steatosis and elevated triglycerides [11, 12]. As a result, direct LXR agonists are unsuitable for clinical treatment of hypercholesterolemia.

Traditional Chinese medicine (TCM), a hallmark of Chinese traditional culture, has been practiced for over 2000 years and is characterized by its independent theoretical framework and extensive clinical knowledge [13]. TCM is increasingly considered an adjunct option for both primary and secondary prevention of ASCVD [14]. Mongolian medicine—an essential part of Mongolian traditional healing—arose through long-term medical experience and has integrated concepts from both TCM and Tibetan medicine [15]. The Baolier capsule (BLEC), classified as a type III Mongolian hypolipidemic preparation and protected by a national patent, is clinically applied for hypercholesterolemia and coronary heart disease [16-19]. Our earlier work demonstrated, through animal studies and network analysis, that BLEC reduces TC, TG, and LDL-C while elevating HDL-C [19]. Yet, the core compounds responsible for cholesterol lowering and the mechanisms through which BLEC prevents AS formation are still not fully defined.

Piperine—the dominant molecule extracted from black pepper (P. nigrum L.) [20]—exhibits numerous pharmacological actions, such as antioxidant, anti-inflammatory, antimicrobial, antitumor, neuroprotective, antihypertensive, antidiabetic, and liver-protective effects [20]. It also enhances the bioavailability of many drugs by decreasing required doses and dosing frequency [21]. In rodent studies, piperine markedly lowers TC, TG, and LDL-C in animals fed a lipid-rich diet [22]. However, the biochemical pathway through which piperine exerts its lipid-modulating activity has not been elucidated.

The present work integrated animal experimentation, transcriptome profiling, and LC–MS/MS to clarify BLEC's anti-AS actions and to identify its major active constituents. First, an AS mouse model was generated, and BLEC's influence on aortic pathology was evaluated. The hepatic transcriptome was then analyzed to map BLEC-induced gene expression alterations. LC–MS/MS was applied to identify BLEC-derived components present in liver tissue. Finally, independent in vivo assays were conducted to verify how piperine—BLEC's principal component—affects hypercholesterolemia and AS. Collectively, this study offers experimental evidence for further exploration of BLEC and piperine in the context of AS treatment and contributes new insights for therapeutic development.

Materials and Methods

Materials

All primary reagents, manufacturers, and equipment specifications are provided in **Table 1**.

Table 1. Key Resources Table

Category	Reagent or Resource	Source	Identifier / Catalog No.
Antibodies			
	Anti-ABCA1 (Rabbit monoclonal)	Proteintech	26564-1-AP
	Anti-ABCG8 (Rabbit monoclonal)	Proteintech	24453-1-AP
	Anti-ABCG5 (Rabbit monoclonal)	Proteintech	27722-1-AP
	Anti-CYP7A1 (Rabbit monoclonal)	Proteintech	18054-1-AP
	Anti-LXRα (Rabbit monoclonal)	Proteintech	14351-1-AP
	Anti-β-actin (Mouse monoclonal)	Proteintech	66009-1-Ig
Drugs and Chemicals			
	Baolier Capsule (BLEC)	Inner Mongolia Mongolian Medicine Joint Stock Co., Ltd.	Z20030129
	Piperine	MedChemExpress	HY-N0144
	Atorvastatin	SUPELCO	PHR1422-1G
	Ezetimibe	SUPELCO	PHR1866-1G
Experimental Models			
	ApoE−/− mice	Gempharmatech	T001458-3
Oligonucleotides			

Control shRNA (sequence: GATCCCCTTCTCCGAACGTGTCACGTT TCAA GAGAACGTGACACGTTCGGAGAATTT TTA)	Sigma-Aldrich	This paper
LXRα shRNA (sequence: GTCATCTTAGAGCCAGAGGAT)	Sigma-Aldrich	This paper
AAV2/8 vector	Obio Technology Co., Ltd	This paper
Commercial Assays and Kits		
Oil Red O staining solution	Yuan Ye	S19039
TRIzol Reagent	Thermo Fisher Scientific	15596026
5× Evo M-MLV RT Master Mix	Accurate Biology (Rui Zhen)	AG11706
2× SYBR Green Pro Taq HS Premix	Accurate Biology (Rui Zhen)	AG11701
Total cholesterol (TC) assay kit	Elabscience	E-BC-K109-M
LDL-C assay kit	Elabscience	E-BC-K205-M
HDL-C assay kit	Elabscience	E-BC-K221-M
Triglyceride (TG) assay kit	Elabscience	E-BC-K261-M
AST assay kit	Nanjing Jiancheng Bioengineering Institute	C010-2-1
ALT assay kit	Nanjing Jiancheng Bioengineering Institute	C009-2-1
Total bile acid (TBA) assay kit	Elabscience	E-BC-K181-M
Phospholipid assay kit	Wako	296–63801
Instruments		
Fluorescence inversion microscope system	Olympus	CellSens Dimension
Blood glucose monitoring system	OneTouch	Ultra Easy
ACQUITY UPLC I-Class Plus system	Waters Corporation	–
Q-Exactive high-resolution mass spectrometer	Thermo Fisher Scientific	–

Preparation of BLEC

To prepare the suspension, 5 g of sodium CMC was dissolved in 1000 mL of ddH_2O and mixed for 12 h at room temperature. The measured quantity of BLEC powder was added to 0.5% CMC–Na, and the mixture was kept at 4°C.

Animals

Ethical approval was obtained from the Animal Ethics Committee of Southern Medical University (Guangzhou, China), approval number 2020-BSGZ-07-01, and all procedures complied with national animal-care guidelines. Environmental conditions were maintained at 20°C ± 2°C, relative humidity 50% ± 20%, under a 12-h light/dark cycle. Male ApoE−/− mice had unrestricted access to food and water and underwent a 1-week acclimatization period. Hepatocyte-specific LXRα knockout was generated via tail-vein delivery of AAV2/8-shLXRα (10^{11} pfu).

Constructing the AS model and experimental groups

Animals were provided with a high-fat diet (containing 15% fat and 1.2% cholesterol) for 8 weeks. They were then randomly assigned to the indicated treatment groups, as noted in the figure legends.

Collection of blood samples, liver tissue, and aorta

Anesthesia was induced using 2–5% isoflurane (2-chloro-2-difluoromethoxy-1-1-1-trifluoroethane) in oxygen/air. Once fully anesthetized, blood was collected. The thoracic and abdominal cavities were opened, the heart exposed, and physiological saline was infused via the left ventricle for whole-body perfusion. Organs—including liver and heart—were harvested, rapidly cooled in liquid nitrogen, and stored at −80°C. Body weight was recorded prior to tissue collection.

Oil red O staining and imaging

After euthanasia, the thoracic and abdominal cavities were opened to assess the extent of AS. The aorta—from the root to the iliac bifurcation—was carefully removed and cut longitudinally. Following staining with a commercially prepared Oil Red O solution, images were captured against a blue background using a digital camera. Oil Red O staining was also applied to cross-sections of the aortic root and to liver samples, and these were imaged using a Fluorescence Inversion Microscope System. The AS load was quantified as aortic lesion area/total aorta area (%) and aortic root lesion area/aortic root cross-sectional area (%).

Transcriptomics analysis

Total RNA was isolated from liver samples. The extraction and library-construction procedures followed previously published methods [23]. Raw RNA-seq reads were processed using a computational workflow. Reads containing ambiguous bases were removed, and the remaining clean reads were aligned to the mm9 mouse reference genome using TopHat v1.4.0, permitting no more than two mismatches. Transcript reconstruction was performed with Cufflinks v1.3.0, using UCSC RefSeq gene annotations. Gene-expression measurements were obtained as FPKM values. Differential-expression testing used DESeq (with biological replicates) via estimateSizeFactors and nbinomTest, or edgeR (when replicates were unavailable). Transcripts with $p < 0.05$ and fold change > 2 were considered significantly altered. Enrichment analyses for Gene Ontology (GO) terms and Kyoto Encyclopedia of Genes and Genomes (KEGG) pathways were carried out with an R-based hypergeometric-distribution package, with $p < 0.05$ indicating significant enrichment.

RNA isolation, reverse transcription, and quantitative real-time PCR

RNA from mouse liver was prepared using Invitrogen TRIzol. cDNA synthesis was performed in a 10-μL reaction using 5× Evo M-MLVRT Master Mix. qPCR was run with 2× SYBR Green Pro Taq HS Premix. Relative gene expression was calculated using the ΔΔCt approach, with ACTIN as the internal reference.

Biochemical assays

Blood glucose was measured from the tail vein using a OneTouch UltraEasy glucometer. Whole blood was obtained via the retro-orbital plexus following established procedures. After clotting for 30 min at room temperature, serum was separated by centrifugation at 1500 g for 10 min. Serum TC, LDL-C, HDL-C, and TG were quantified using commercial assay kits.

For hepatic lipid measurements, liver tissue lipids were extracted with a methanol–chloroform (2:1, v/v) mixture, and the resulting extracts were assayed for TC and TG. Liver-injury markers AST and ALT were measured using dedicated commercial kits.

Gallbladder bile was collected after a 4-h fast, and its volume was measured using a p10 pipette tip. For bile composition analysis, 5 μL of bile was diluted with 45 μL Milli-Q water and extracted using 200 μL of chloroform–methanol (2:1). Organic and aqueous layers were evaporated and re-dissolved in ethanol or water. The organic phase was tested for TC and total bile acids (BAs), while biliary phospholipids were measured using WAKO LabAssay kits.

Feces were collected over 3 days, lyophilized, and weighed. Total fecal BAs were extracted with methanol, and fecal lipids were isolated with methanol–chloroform (2:1, v/v). All biochemical data were processed using Microplate Manager 6 / SoftMax Pro v7.1.

Extraction of BLEC components from liver samples

Frozen liver tissues stored at −80°C were thawed on ice. For each sample, 100 mg of tissue was transferred to 1.5-mL Eppendorf tubes and mixed with 600 μL methanol–acetonitrile (4:1, v/v) containing 4 μg/mL L-2-chlorophenylalanine. Samples were vortexed for 1 min, sonicated on ice for 10 min, and then incubated at −40°C overnight. Extracts were centrifuged at 12000 rpm, 4°C for 10 min, and subsequently kept at −40°C for 2 h.

A 500-μL aliquot of supernatant was transferred to vials for drying. Dried materials were reconstituted in 300 μL methanol–acetonitrile–water (2:1:1, v/v/v), vortexed for 30 s, sonicated for 3 min, and left again at −40°C overnight. The next day, samples were centrifuged at 12000 rpm, 4°C for 10 min, and 150 μL of the final supernatant was prepared for analysis.

Extraction of BLEC components

Chinese herbal samples were precisely measured to 100 mg and placed into 1.5-mL EP tubes. A total of 1 mL of a methanol–water mixture (1:1, v/v) containing 4 μg/mL of L-2-chlorophenylalanine was added, then heated to roughly 80 °C to promote dissolution, followed by 2 minutes of vortex mixing. Afterward, the mixture was centrifuged at 12,000 rpm for 10 minutes at 4 °C. The clear supernatant was passed through a 0.22-μm organic membrane filter, diluted fivefold with the same methanol–water solution (1:1, v/v, with 4 μg/mL L-2-chlorophenylalanine), and 200 μL of the resulting extract was transferred into wide-bore injection vials for analysis. A quality control (QC) sample was generated by pooling equal volumes of centrifuged supernatants from both medicated and prototype samples so that the instrument-measured concentrations remained consistent across groups.

LC–MS/MS analysis

Metabolomic profiling was carried out by Shanghai Luming Biological Technology Co., Ltd. (Shanghai, China). An ACQUITY UPLC I-Class Plus system coupled with a Q-Exactive mass spectrometer featuring a heated ESI source was employed for both positive and negative ion detection. Chromatographic separation was used with an ACQUITY UPLC HSS T3 column (1.8 μm, 2.1 × 100 mm). The binary mobile phase consisted of (A) water with 0.1% formic acid (v/v) and (B) acetonitrile with 0.1% formic acid (v/v), applied under this gradient sequence: 0.01 min: 5% B; 2 min: 5% B; 4 min: 30% B; 8 min: 50% B; 10 min: 80% B; 14 min: 100% B; 15 min: 100% B; 15.1 min: 5% B; 16 min: 5% B. The flow rate was maintained at 0.35 mL/min, the column was set to 45 °C, and samples were stored at 4 °C throughout. Each injection volume was 5 μL.

Mass spectra were collected from m/z 100–1200. Instrument resolution was set to 70,000 for full-scan MS and 17,500 for HCD MS/MS. Collision energies were adjusted to 10, 20, and 40 eV. Ionization parameters included spray voltages of 3800 V (positive mode) and 3000 V (negative mode), sheath gas at 35 arbitrary units, auxiliary gas at 8 arbitrary units, capillary temperature at 320 °C, auxiliary gas heater at 350 °C, and an S-lens RF level of 50.

LC–MS/MS data preprocessing

Raw chromatographic–mass spectrometric outputs were handled in Progenesis QI 3.0 (Nonlinear Dynamics, Newcastle, UK), which was used for baseline correction, feature selection, integration, retention-time adjustment, peak alignment, and normalization. Key settings included a precursor tolerance of 5 ppm and a fragment tolerance of 10 ppm. Identification relied on accurate m/z values, MS/MS fragment ions, and isotopic patterns with reference to the LuMet-TCM, Animal_DB, and Herb databases. Compounds were accepted as identified when their total score exceeded 50, or when the total score was >40 with a secondary-match score above 50. Components with an FC value greater than 10 in comparisons between treated serum (administration) and blank serum (control) were considered absorbed constituents. The cumulative relative peak area of all detected metabolites was normalized to 100%, creating a merged quantitative-qualitative matrix from both ionization modes. This matrix contained the full dataset used for subsequent statistical analysis. For each characterized TCM compound and circulating component, extracted-ion chromatograms (EICs), annotated MS2 mirror spectra, and classification-based pie charts of compound abundance and count were produced. To further validate the assigned structures, EICs and MS/MS spectra of every entry in the matrix were re-examined, and fragment ions along with their structural annotations were confirmed manually to ensure accurate identification.

Identification criteria

Compound identification relied on three main parameters:

1. The difference between the observed retention time and that recorded for the reference standard in the database had to fall within ±0.2 min.
2. The mass error for the precursor ion (MS1) was required to be ≤5 ppm.
3. A comparison of the acquired MS2 spectrum with the corresponding reference fragmentation spectrum.

When MS2 fragment information was unavailable, identification was verified by matching the standard compound’s retention time and confirming that the molecular ion mass error was within acceptable limits.

Statistical analysis

The sample size selection in this work drew upon earlier studies and fundamental statistical needs rather than depending solely on preset calculations. Each "n" value represented a single mouse in the in vivo assays, ensuring adequate biological representation. Results were consistently reported as mean ± standard deviation. All analyses were performed using GraphPad Prism version 8. Depending on the nature of the comparison, we used one-way ANOVA with Tukey's post hoc test for multiple-group evaluations, unpaired two-tailed Student's t-tests for pairwise assessments, or two-way ANOVA followed by Šídák's post hoc test, as indicated in the figure captions. A significance level of $P < 0.05$ was applied throughout to validate the robustness of the findings.

Results and Discussion

BLEC reduces AS progression in vivo

As in our earlier work [10], ApoE−/− mice were provided either standard chow or an HFD for 12 weeks and subsequently given BLEC (75 mg/kg/day) or ddH2O (control) by gavage over a 4-week period to evaluate BLEC's influence on AS development. At termination, lesion formation in the aortic roots and en-face preparations was examined. Both analyses demonstrated that BLEC-treated ApoE−/− mice on the HFD exhibited notably smaller lesion areas than untreated mice, while chow-fed groups showed no substantial differences **(Figures 1a–1d)**.

Oil Red O staining of en-face aortic surfaces showed a 23.3% reduction in lesion area after BLEC treatment relative to controls. Quantification of Oil Red O-stained cross-sections of the aortic root further verified BLEC's benefit, revealing a 25.1% decrease in plaque area in BLEC-treated mice compared with untreated animals. Together, these findings show that BLEC slows AS progression in HFD-fed ApoE−/− mice.

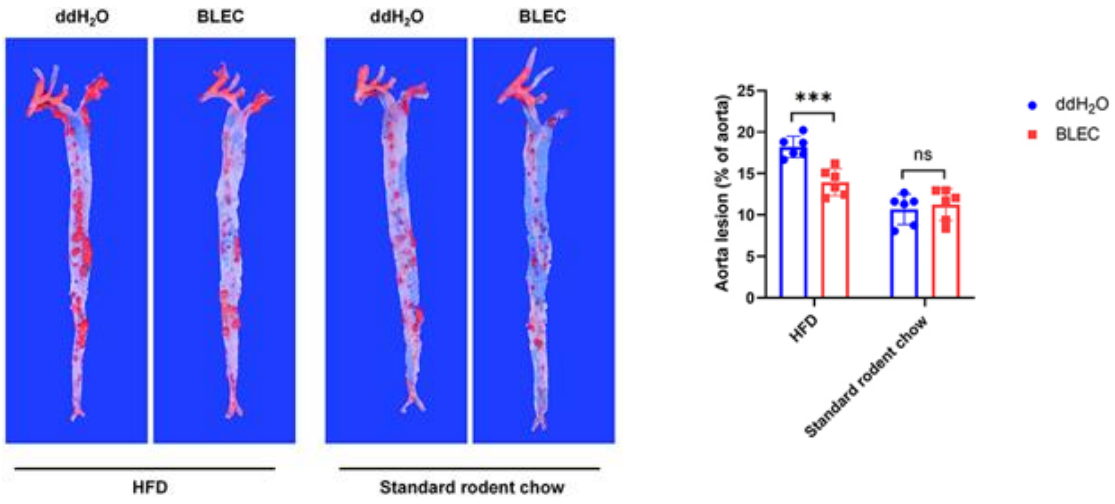

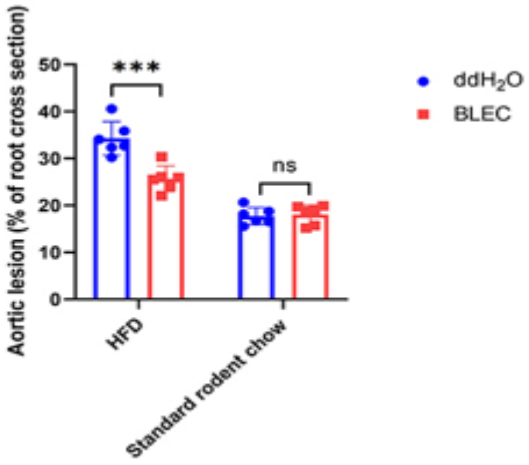

d)

Figure 1. BLEC decreases AS development in vivo. (a) Oil Red O staining of aortas from ApoE−/− mice fed chow or HFD for 8 weeks and treated with BLEC (75 mg/kg/day) or ddH2O for 4 weeks. (b) Quantified en-face lesion areas corresponding to (a). (c) Oil Red O staining of aortic cross sections under the same conditions. Scale: 200 μm. (d) Quantified cross-sectional lesion sizes for (c). Data = mean ± SD, N = 6 mice per group. ***P < 0.001, unpaired two-tailed t-test.

BLEC influences serum lipid profiles in vivo

Given that BLEC reduced plaque size in ApoE−/− mice, and considering the central role of cholesterol imbalance in AS, we next assessed serum lipid levels in HFD-fed animals. Both treatment and control groups appeared outwardly normal **(Figures 2a–2d)**. BLEC administration led to reductions in serum TC (27.4%), LDL-C (39.9%), and TG (26.2%) compared with control mice **(Figures 2e–2g)**. In contrast, HDL-C levels rose by 38.7% in BLEC-treated animals **(Figure 2h)**.

Similarly, hepatic TC and TG levels were lower in BLEC-treated mice than in controls **(Figures 2i–2j)**. Consistent with these biochemical findings, BLEC markedly diminished hepatic lipid droplet accumulation with no signs of liver injury **(Figures 2k–2m)**. Collectively, these data suggest that BLEC mitigates AS partly by correcting hypercholesterolemia.

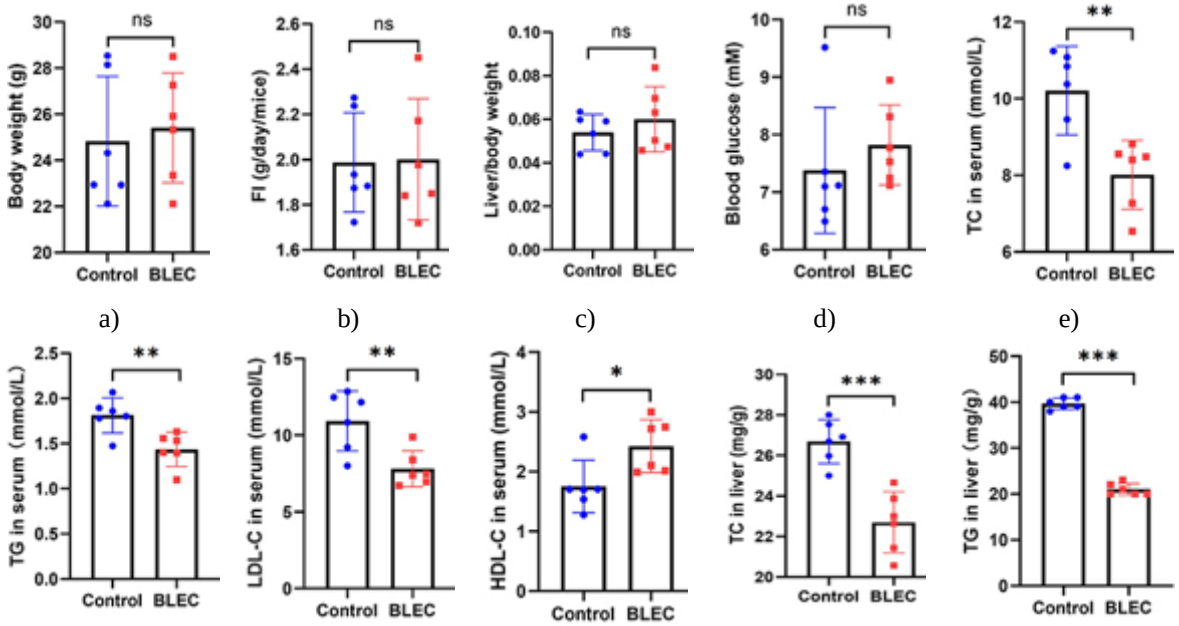

a) b) c) d) e)

f) g) h) i) j)

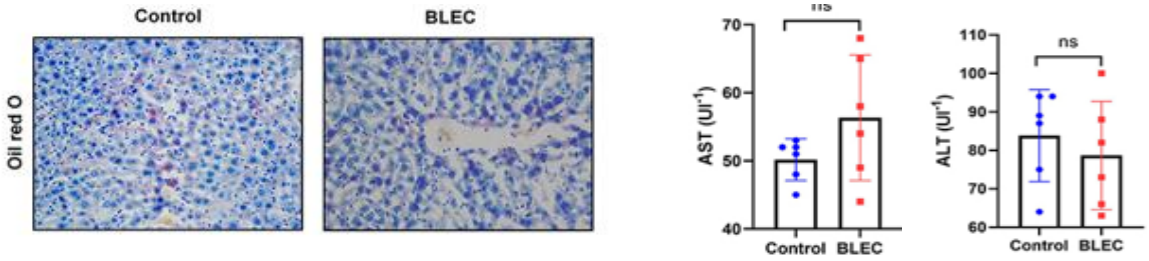

k) l) m)

Figure 2. Regulation of circulating lipids by BLEC in vivo.
ApoE−/− mice were maintained on an HFD for 8 weeks and then orally given either BLEC (75 mg/kg/day) or ddH2O for an additional 4 weeks. The following parameters were recorded: (a) body mass, (b) food intake (FI), (c) liver-to-body mass ratio, (d) blood glucose, (e) serum TC, (f) serum TG, (g) serum LDL-C, (h) serum HDL-C, (i) hepatic TC, (j) hepatic TG, and (k) Oil Red O–stained liver slices (scale = 100 μm). Panels (l) and (m) show serum AST and ALT, respectively. Values represent mean ± SD for N = 6 animals per group. Statistical significance: *P < 0.05, **P < 0.01, ***P < 0.001 by unpaired two-tailed t-test.

Transcriptome profiling identifies molecular pathways influenced by BLEC during cholesterol control

To explore the molecular shifts produced by BLEC, we examined transcriptomic alterations between treatment groups. Because hepatic tissue governs cholesterol turnover, liver samples were subjected to RNA-based analysis. Using a cutoff of ≥2.0-fold difference and P ≤ 0.05 (Student's t-test), the comparison yielded 1349 transcripts with significant variation. Of the 1349 transcripts, 660 showed increased expression, while 689 were reduced, as displayed in the volcano plot.

GO and KEGG annotations were used to determine the biological context of these transcript changes. GO mapping indicated that the altered genes were primarily enriched in biological processes linked to lipid and fatty-acid handling, in cellular-component terms associated with mitochondrial structures, and in molecular-function categories involving oxidoreductases and ABC-type transporters. **Figure 3a** summarizes the enriched GO terms. KEGG analysis identified 45 pathways with significant enrichment, and the 20 most prominent ones are displayed in **Figure 3b**.

A chord-diagram approach was then applied to highlight transcripts positioned at the intersection of three key themes: fatty-acid/lipid metabolism, ABC-transporter activity, and bile secretion. This analysis highlighted ABCA1, ABCG5, ABCG8, and CYP7A1 as central components of these pathways **(Figures 3c and 3d)**, all of which were strongly upregulated. Overall, these data suggest that BLEC counteracts hypercholesterolemia and AS by elevating genes responsible for cholesterol export and mobilization.

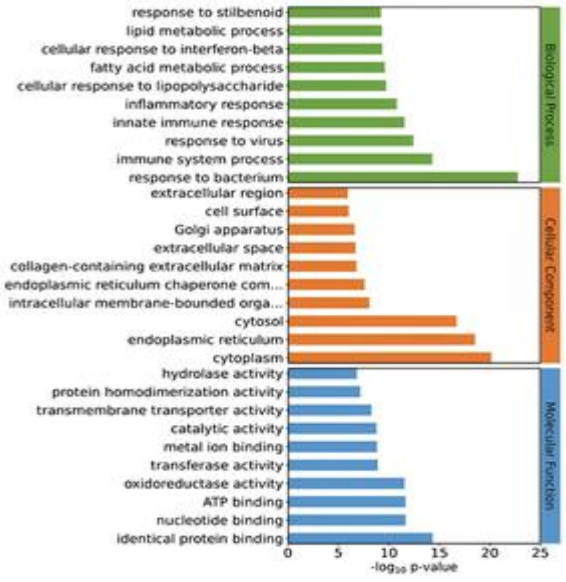

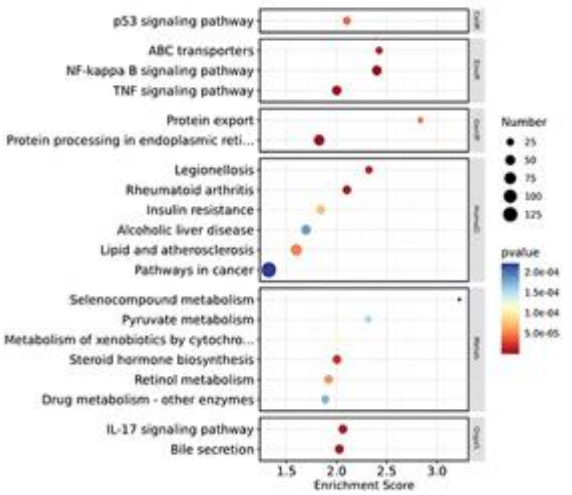

a) b)

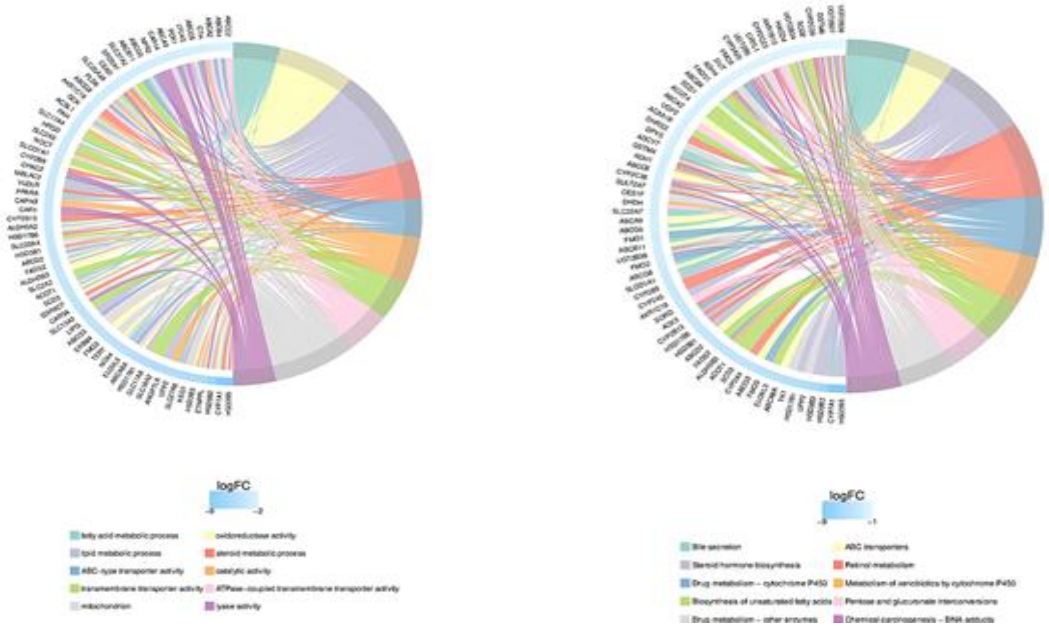

c) d)

Figure 3. Transcriptomic evaluation of BLEC-related pathways.
(a) GO enrichment patterns.
(b) KEGG pathway enrichment.
(c) GO-based chord diagram of altered transcripts.
(d) KEGG-based chord diagram of altered transcripts.

BLEC enhances hepatic cholesterol elimination

To determine whether BLEC promotes the removal of cholesterol through biliary routes, we examined bile parameters. BLEC-treated animals displayed higher bile output along with elevated concentrations of gallbladder cholesterol and bile acids **(Figures 4a-4c)**. Total biliary cholesterol increased by 73.9%, and total bile acids rose by 153.4% relative to controls **(Figures 4d and 4e)**. BLEC also reduced the cholic-acid/muricholic-acid ratio and produced a slight elevation in biliary phospholipids **(Figures 4f-4h)**. Because cholic acid enhances intestinal absorption of cholesterol more effectively than muricholic acid, this shift in bile-acid composition may help explain the lower systemic cholesterol levels. As expected, bile from control mice remained clear, whereas bile from BLEC-treated mice was visually opaque **(Figure 4i)**.

Consistent with these findings, hepatic expression of ABCA1, ABCG5, ABCG8, CYP7A1, and LXRα was markedly increased **(Figures 4j-4k)**, aligning with the elevated bile cholesterol/BA content and reduced lipid burden in blood and liver. Taken together, the data support that BLEC alleviates hypercholesterolemia and AS predominantly by accelerating cholesterol excretion through the liver.

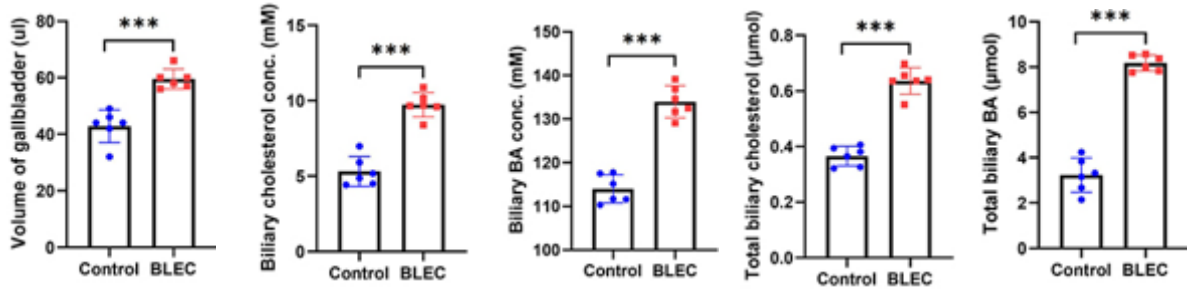

a) b) c) d) e)

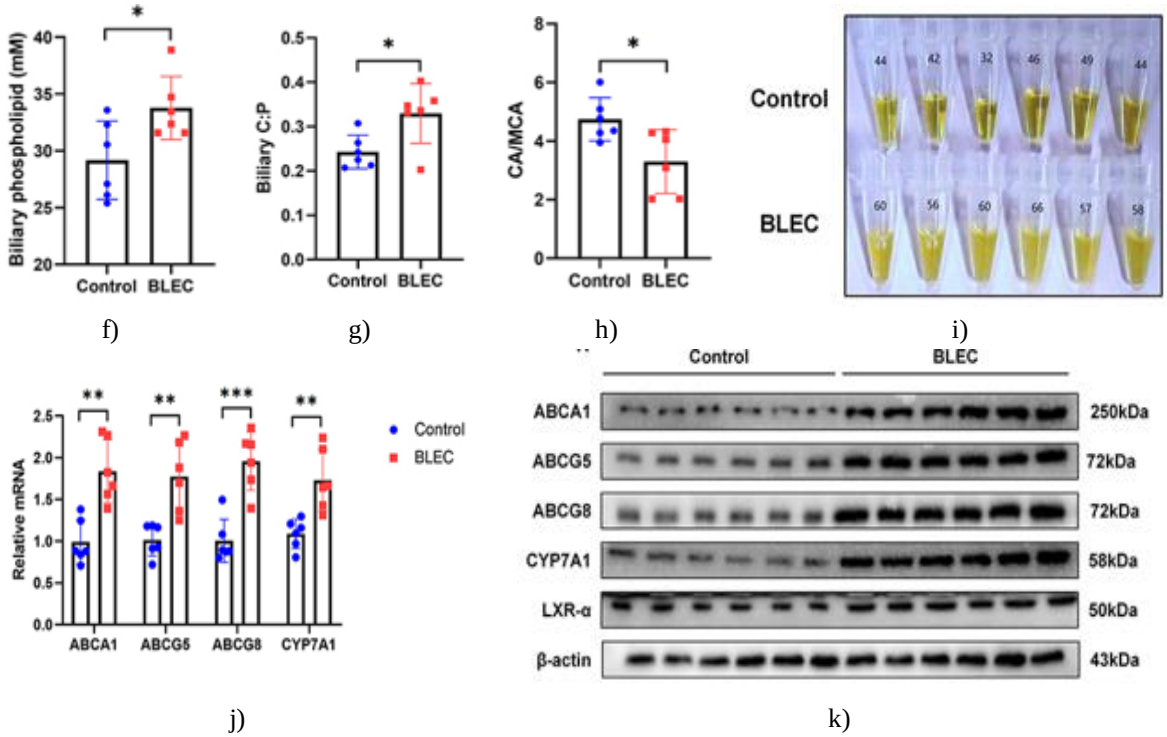

Figure 4. BLEC enhances cholesterol elimination.

ApoE−/− mice maintained on a high-fat diet (HFD) for 8 weeks were subsequently given BLEC (75 mg/kg/day) or ddH_2O by oral gavage for an additional 4 weeks. (a) Gallbladder bile volume. (b) Cholesterol levels in bile. (c) Concentrations of bile acids. (d) Total biliary cholesterol output. (e) Overall, biliary bile acids. (f) Phospholipid content in bile. (g) Ratio of cholesterol to phospholipids (C:P). (h) Proportion of cholic acid (CA) relative to muricholic acid (MCA). (i) Representative bile photographs. (j) Hepatic gene expression measured using RT-qPCR. (K) Liver protein expression assessed by Western blotting. Values are presented as mean ± SD, with N=6 mice per group. Statistical significance was determined using an unpaired two-tailed t-test: *P<0.05, **P<0.01, ***P<0.001.

LC-MS/MS profiling of BLEC constituents involved in cholesterol excretion and anti-AS activity

To further verify the components of BLEC responsible for promoting cholesterol disposal and mitigating AS, the BLEC extract was subjected to LC-MS/MS. Compound identities were confirmed or tentatively assigned based on MS and MS/MS fragmentation patterns, supported by published reports and spectral databases (MassBank, NIST, etc.). A total of 1611 notable constituents were detected. Among all chemical categories, flavonoids, terpenes, and phenylpropanoids showed the greatest diversity at 17.76%, 17.56%, and 14.33%, respectively **(Figure 5a)**. In contrast, classes with the highest content were terpenes (26.57%), alkaloids (15.62%), and steroids (14.85%) **(Figure 5b)**. Within the ten most abundant individual molecules, piperine accounted for the largest share at 27.45% **(Figure 5c)**.

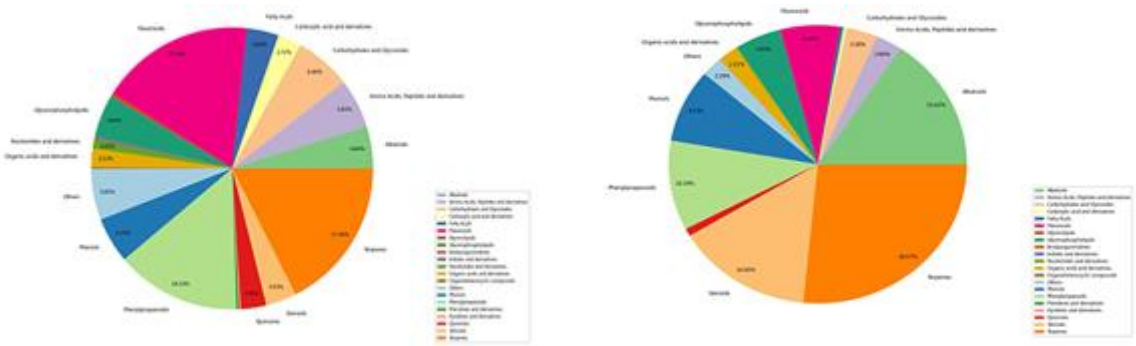

a) b)

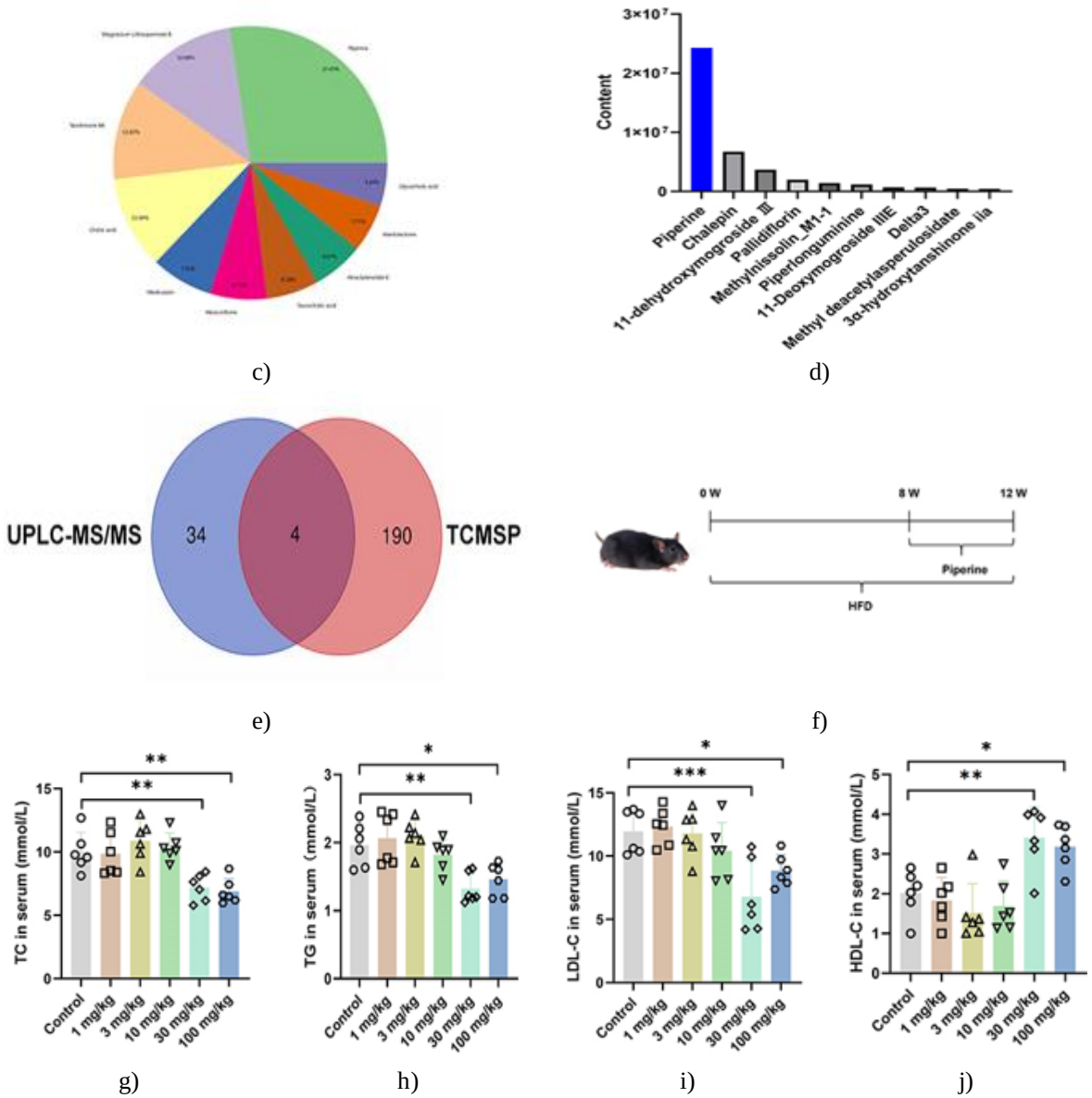

c) d) e) f) g) h) i) j)

Figure 5. UPLC-MS/MS characterization of BLEC constituents linked to cholesterol excretion and anti-AS effects.

(a–c) Category distribution (a), relative content distribution (b), and content-based ranking of the top ten molecules (c).

(d) Ten most abundant prototype compounds detected in the livers of BLEC-treated mice.

(e) Overlapping components identified between liver-detected molecules and those predicted as active constituents based on the TCMSP database.

(f) Experimental workflow for the mouse study.

(g–j) ApoE−/− mice fed HFD for 8 weeks were treated with piperine (0, 1, 3, 10, 30, 100 mg/kg/day) or ddH₂O for 4 weeks. Serum TC (g), TG (H), LDL-C (i), and HDL-C (j) are shown. Data represent mean ± SD for N=6 per group, analyzed by one-way ANOVA (*P<0.05, **P<0.01, ***P<0.001).

Pharmacological studies indicate that orally administered TCM formulations distribute to target tissues, where their active components exert direct biological effects. To identify BLEC-derived substances actively regulating hepatic cholesterol pathways, mice were treated with BLEC (75 mg/kg/day) for seven days. Water was provided throughout, and food was withdrawn for 12 h before the final administration. Livers were collected 4 h after the last dose. Ions with prominent signals in BLEC-treated samples but negligible or absent in controls were screened to eliminate interference from endogenous metabolites. Structural assignments were made using MS/MS fragmentation and reference studies of BLEC constituents. In total, 38 prototype molecules were identified, with

piperine being the most abundant **(Figure 5d)**. When comparing active compounds predicted from TCMSP with those detected in the liver, piperine, tanshinone IIa, neocryptotanshinone, and piperlonguminine overlapped **(Figure 5e)**, supporting piperine's central role in BLEC's activity profile.

Next, piperine's lipid-modulating effects were tested in hyperlipidemic ApoE−/− mice. Animals consumed HFD for 12 weeks prior to receiving piperine daily (1, 3, 10, 30, or 100 mg/kg) or vehicle for 4 weeks via gastric gavage **(Figure 5f)**. A robust, dose-responsive decrease in circulating lipid levels was observed in piperine-treated groups **(Figures 5g–5j)**. The 30 mg/kg dose produced the most pronounced improvement. Collectively, these findings establish piperine as the principal bioactive component of BLEC responsible for ameliorating hyperlipidemia and AS.

Piperine elevates cholesterol disposal and depends on LXRα

ABCA1, ABCG5, ABCG8, and CYP7A1 are transcriptional targets primarily governed by liver X receptor α (LXRα). With this in mind, we examined whether piperine enhances hepatic cholesterol clearance and whether these actions require LXRα signaling. To do so, we generated liver-specific LXRα knockout ApoE−/− mice (TKO) by delivering AAV through the tail vein. Both TKO and ApoE−/− wild-type mice (WT) were maintained on an HFD for 8 weeks and then given piperine (30 mg/kg/day) or ddH_2O by gavage for 4 weeks. Body mass, dietary intake, and glucose readings were comparable across groups. However, deletion of LXRα resulted in severe hepatic lipid droplet accumulation, hepatocyte ballooning, and elevated AST and ALT **(Figure 6a)**. Piperine markedly lowered hepatic fat levels and reduced serum TC and TG, but these improvements were fully lost when LXRα was removed **(Figures 6b–6e)**. LDL-C declined, while HDL-C rose in the piperine group compared with controls **(Figures 6f and 6g)**. Total cholesterol in the bile approximately doubled after piperine treatment relative to the control, but fell back to baseline in piperine-treated TKO animals **(Figures 6h–6m)**. Fecal cholesterol increased by 118.0% with piperine, an effect absent in LXRα-deficient mice **(Figure 6n)**. These findings correspond with changes in ABCA1, ABCG5, ABCG8, and CYP7A1 expression: ABCG5/G8 transfers cholesterol into bile for elimination in feces, while ABCA1 delivers cholesterol to HDL **(Figures 6o–6r)**. Collectively, these results show that piperine is the dominant active molecule in BLEC for improving hypercholesterolemia and AS, and its metabolic actions rely on LXRα.

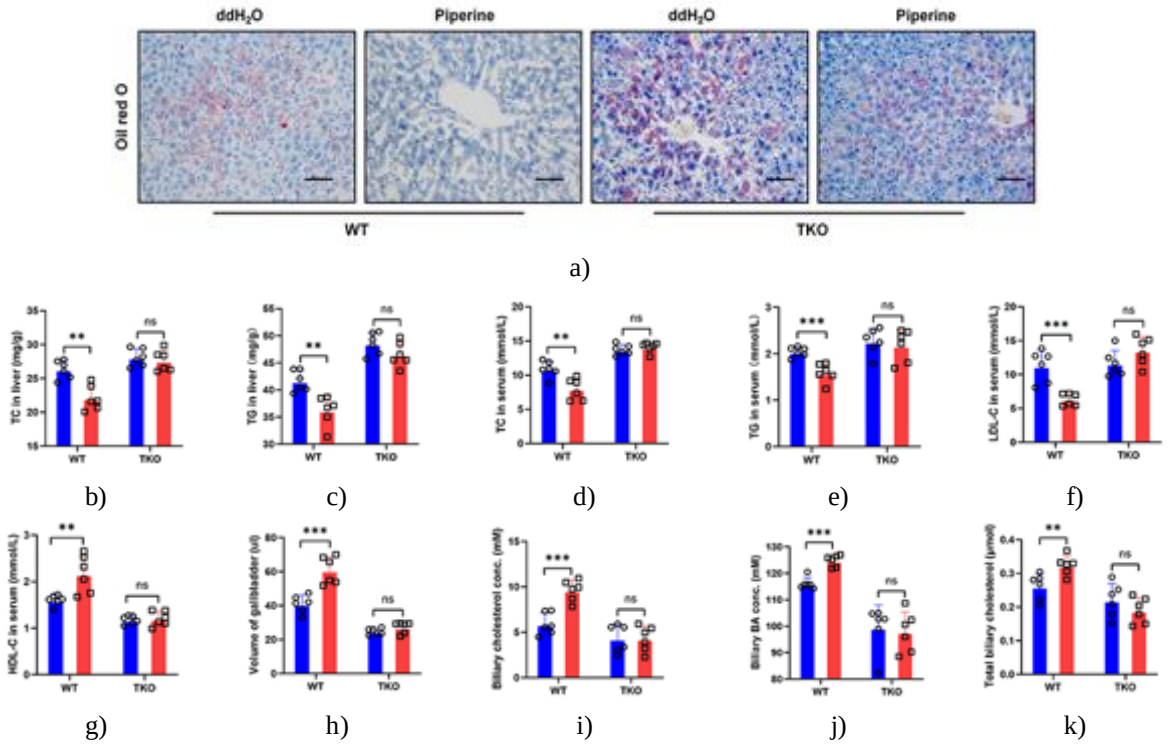

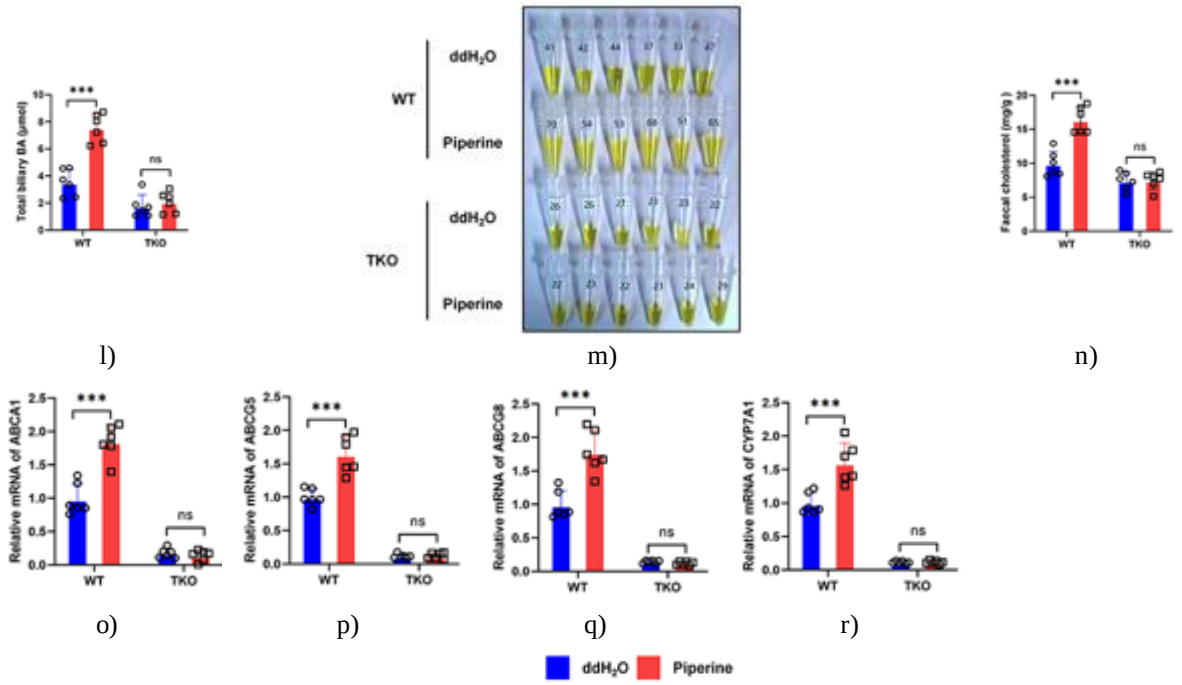

Figure 6. Piperine enhances cholesterol removal in an LXRα-dependent manner.
ApoE−/− mice with liver-targeted LXRα knockout (TKO) and ApoE−/− wild-type mice (WT) were fed HFD for 8 weeks and then received piperine (30 mg/kg/day) or ddH₂O by oral gavage for 4 weeks.
(a) Oil Red O staining of liver sections. Scale bar = 100 μm. (b) Serum TC. (c) Serum LDL-C. (d) Serum TG. (e) Serum HDL-C. (f) Hepatic TC. (g) Hepatic TG. (h) Gallbladder bile volume. (i) Biliary cholesterol concentration. (j) Biliary bile acid concentration. (k) Total biliary cholesterol. (l) Total biliary bile acids. (m) Representative bile photos. (n) Fecal cholesterol. (o–r) Hepatic ABCA1 (o), ABCG5 (P), ABCG8 (q), and CYP7A1 (r) mRNA measured by RT-qPCR.
Data are mean ± SD, N = 6 per group. **P < 0.01; ***P < 0.001 via unpaired two-tailed t-test.

Piperine acts synergistically with statins and ezetimibe

To determine whether piperine enhances the actions of established lipid-modifying therapies, we compared its effects with atorvastatin and ezetimibe (EZ). Administering piperine or atorvastatin separately lowered TC and TG to a comparable extent in ApoE−/− mice. When both agents were given together, however, the decline in circulating and hepatic lipid content was far more pronounced **(Figures 7a–7d)**. Body mass and general metabolic indicators did not differ between treatment groups.

Independent of atorvastatin exposure, piperine increased the expression of ABCA1, ABCG5, ABCG8, and CYP7A1 **(Figures 7e–7h)**. In line with these transcriptional changes, piperine consistently elevated total biliary cholesterol, total biliary BAs, and fecal cholesterol in ApoE−/− mice, whereas atorvastatin alone produced no measurable effect on these outputs **(Figures 7i–7k)**. Serum AST and ALT remained comparable across all conditions **(Figures 7l–7m)**.

We next tested piperine in combination with EZ. In ApoE−/− mice, piperine's activity was essentially unchanged by the presence or absence of EZ **(Figures 5n–5z)**. In WT animals, piperine and EZ together reduced serum and hepatic TC and TG more effectively than when either drug was administered alone **(Figure 7n–7q)**. Piperine still increased biliary cholesterol, biliary BAs, and fecal cholesterol without causing detectable hepatic injury, even during EZ co-treatment **(Figures 5r–5v)**. Under EZ exposure, however, piperine did not raise ABCA1, ABCG5, ABCG8, or CYP7A1 transcript levels **(Figures 7w–7z)**.

Crucially, piperine attenuated AS whether used by itself, paired with statins or EZ, or delivered alongside both. The triple regimen provided the strongest suppression of AS development **(Figure 8)**. These observations collectively suggest that piperine has meaningful therapeutic value for hypercholesterolemia and AS.

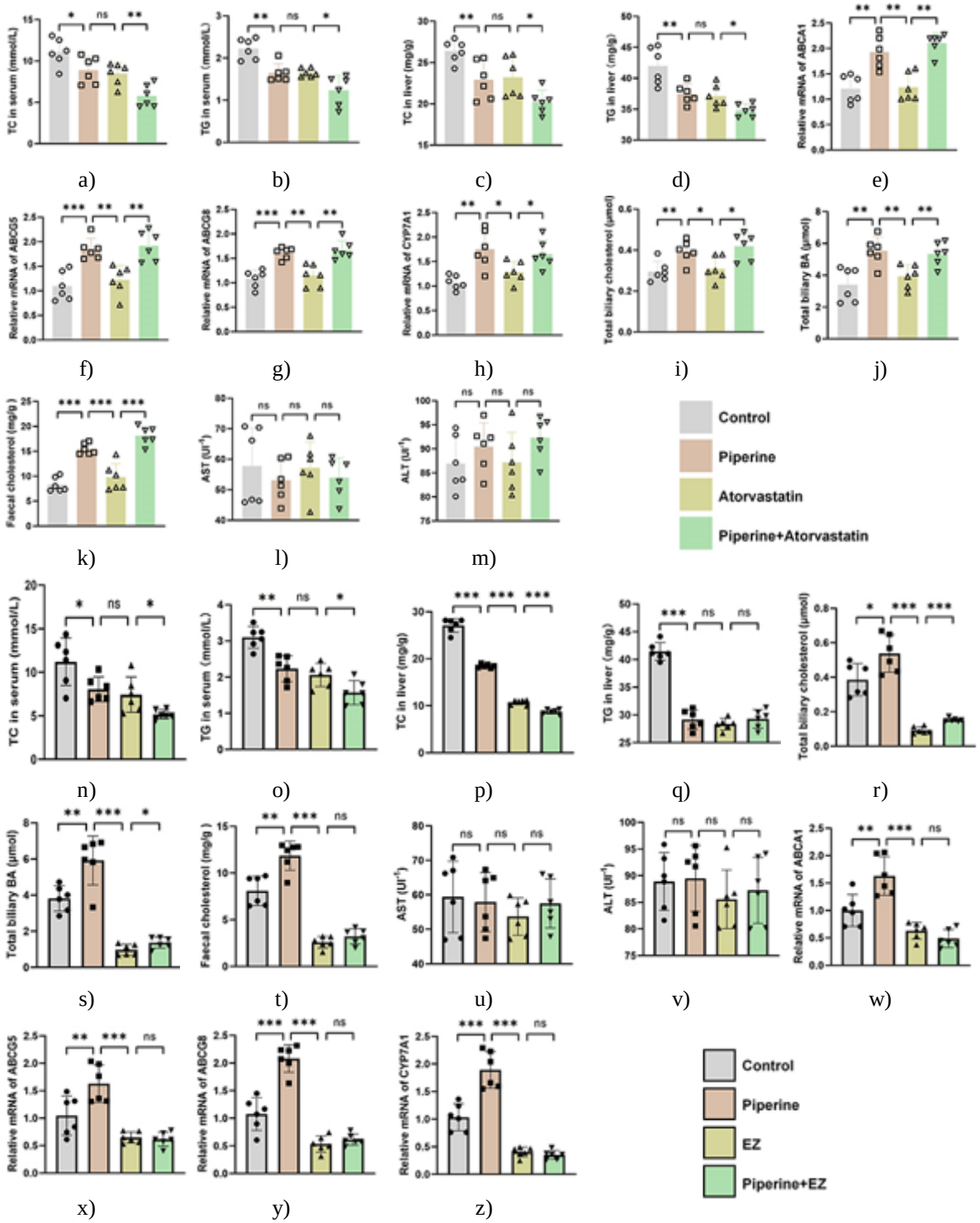

Figure 7. Cooperative Effects of Piperine with Statins/EZ on Lipid Indices

Eight-week-old male ApoE−/− mice were randomly assigned to groups, maintained on an HFD for 8 weeks, and then administered ddH2O, piperine (30 mg/kg/day), atorvastatin (30 mg/kg/day), or both agents for 4 weeks by gavage.

(a) Serum TC. (b) Serum TG. (c) Hepatic TC. (d) Hepatic TG. (e–h) Liver expression of ABCA1 (e), ABCG5 (f), ABCG8 (g), CYP7A1 (h) via RT-qPCR. (i) Total biliary cholesterol. (j) Total biliary BAs. (k) Fecal cholesterol. (l) Serum AST. (m) Serum ALT.

A separate cohort of 8-week-old male ApoE−/− mice underwent the same dietary induction and received ddH2O, piperine (30 mg/kg/day), EZ (10 mg/kg/day), or piperine plus EZ for 4 weeks.

(n) Serum TC. (o) Serum TG. (p) Hepatic TC. (q) Hepatic TG. (r) Total biliary cholesterol. (s) Total biliary BAs. (t) Fecal cholesterol. (u) Serum AST. (v) Serum ALT. (w–z) ABCA1 (w), ABCG5 (x), ABCG8 (y), and CYP7A1 (z) expression levels determined by RT-qPCR.
Values are reported as mean ± SD for N = 6 mice/group.
*P < 0.05, **P < 0.01, ***P < 0.001 using one-way ANOVA.

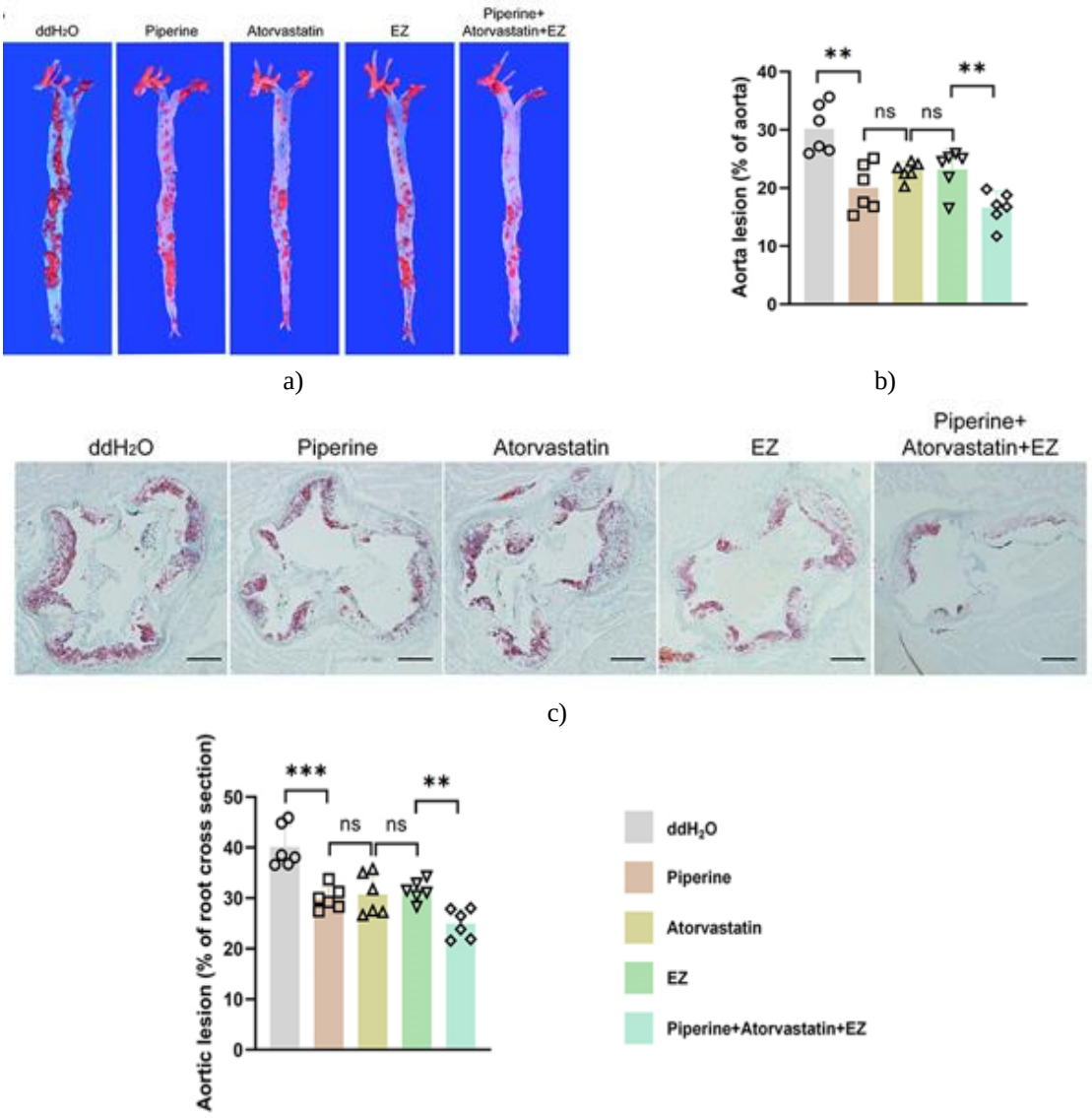

a) b)

c)

d)

Figure 8. Piperine Acts Additively with Statins and Ezetimibe in Limiting AS
(a) Oil Red O staining of the aorta from ApoE−/− mice maintained on an HFD for 8 weeks, followed by 4 weeks of oral treatment with ddH₂O, piperine (30 mg/kg/day), atorvastatin (30 mg/kg/day), ezetimibe (EZ, 10 mg/kg/day), or a combination of piperine + atorvastatin + EZ.
(b) Quantitative analysis of aortic surface lesions corresponding to panel (a).
(c) Oil Red O staining of aortic root cross-sections from mice receiving the same treatments. Scale bar: 200 μm.
(d) Quantification of lesion area in aortic root sections from mice as in (c).
Values represent mean ± SD, N = 6 per group. P < 0.01, ***P < 0.001 via one-way ANOVA.

Our findings demonstrate that BLEC markedly lowered circulating cholesterol and suppressed the development of AS. Transcriptome profiling indicated that BLEC primarily influences pathways involved in hepatic cholesterol elimination, while UPLC-MS/MS data identified piperine as the principal bioactive compound responsible for

these actions. Follow-up studies in vivo verified that piperine enhances hepatic cholesterol disposal by driving the expression of efflux-related genes (ABCA1, ABCG5, ABCG8, and CYP7A1) through LXRα activation. Taken together, these results support the substantial clinical potential of piperine.

Because the rigid cyclopentanoperhydrophenanthrene ring system makes cholesterol difficult for the body to break down [3-24], promoting its excretion—similar to how SGLT2 inhibitors increase urinary glucose elimination to improve cardiometabolic outcomes [25]—represents a desirable strategy for lipid reduction. Yet, no clinically accepted agents explicitly designed to boost cholesterol excretion exist. Mongolian medicine, an important branch of traditional Chinese medicine, emphasizes improving the liver's ability to "separate the essence of blood from impurities" to alleviate AS [26], a concept that aligns closely with the modern understanding that accelerating cholesterol clearance protects against AS. Our study confirms that BLEC enhances cholesterol disposal, reduces circulating lipid levels, and slows atherosclerotic progression. Identifying key components within complex herbal preparations is essential for advancing TCM modernization, ensuring reliable therapeutic effects, and increasing global acceptance of these formulations [27]. Our analysis establishes piperine as the dominant agent in BLEC responsible for its lipid-lowering and anti-AS properties.

Piperine—a biologically active alkaloid derived from species such as Piperis Fructus and Piperis Longi Fructus—has gained attention for its ability to reduce lipid levels and inhibit foam cell formation, thereby limiting AS [28-30]. Studies in hyperlipidemic rats have shown that piperine significantly decreases serum TC and TG, improving dyslipidemia [22, 28, 29]. Piperine and related molecules (e.g., piperlongumine, GBN) also display antioxidant, anti-inflammatory, antineoplastic, anticonvulsant, and immune-modulatory actions—activities linked to AS pathology—beyond their lipid-regulating effects [31-36]. Despite these benefits, direct in vivo evidence for piperine's impact on AS has been scarce. Clinical translation is further complicated by two major issues: (1) its relatively high toxicity, which limits broader application [37], and (2) unresolved pharmacokinetics regarding absorption, distribution, metabolism, and elimination, all requiring deeper investigation [38], Additionally, the precise lipid-modifying pathways engaged by piperine have not been comprehensively defined. Our work shows that piperine acts through LXRα to exert its lipid-lowering and anti-atherosclerotic actions. Moreover, it performs effectively when administered alongside statins or EZ in reducing cholesterol burden and mitigating AS.

Although piperine exhibits dose-dependent benefits, concerns regarding its toxicity must not be overlooked. Future studies should prioritize strategies to minimize piperine-related adverse effects.

LXRα, recognized as a central transcriptional regulator of lipid homeostasis, has become a major focus due to its involvement in cholesterol handling and transport, offering new insights for addressing hypercholesterolemia and AS. LXRα modulates numerous genes in a tissue-specific fashion, influencing cholesterol uptake, movement, removal, and elimination, acting as an essential sensing system for maintaining systemic cholesterol stability [11, 12]. Evidence indicates that stimulating LXRα markedly enhances reverse cholesterol transport— the pathway through which surplus intracellular cholesterol is transferred via HDL to the liver for metabolism and elimination—thereby suppressing the initiation and progression of AS. During this mechanism, LXRα boosts the expression of cholesterol efflux–associated proteins, including ABCA1, ABCG1, ABCG5/G8, and CYP7A1, facilitating cholesterol transfer from peripheral organs to the liver and decreasing intestinal dietary cholesterol absorption [10, 39]. Despite these advantages, the clinical translation of LXRα-based therapies still confronts obstacles. Activation of LXRα can elevate genes involved in fatty acid synthesis, contributing to liver lipid accumulation and rises in TG levels [11, 12]. This side effect limits the direct therapeutic use of LXRα agonists for hypercholesterolemia. Additionally, variations have been noted among different LXRα agonists in animal studies, with some increasing TC and TG, while others raise only HDL-C [11, 12]. Such differences demonstrate that further refinement of agonist selectivity and mechanistic understanding is still required. Our study demonstrates that piperine activates LXRα, enhances cholesterol elimination, lowers TC, TG, and LDL-C, and simultaneously prevents liver steatosis. Therefore, piperine represents a promising cholesterol-lowering and anti-AS agent with strong clinical applicability.

Nonetheless, this work includes several constraints. First, although our multi-omics and molecular experiments confirmed piperine as the principal active constituent of BLEC and used doses comparable to those standardly applied in animal research, these doses exceed those typically used clinically. Additional pharmacologic and safety investigations are required to determine suitable dose ranges for human application. Second, although we verified that piperine enhances hepatic cholesterol excretion and counters AS through LXRα activation without triggering steatosis, the precise pathway through which piperine activates LXRα remains unresolved.

Conclusion

Overall, our findings show that BLEC and piperine mitigate atherosclerosis by modulating lipid metabolism. Mechanistically, both activate LXRα, increasing the expression of genes involved in cholesterol efflux, thereby accelerating cholesterol removal, lowering circulating cholesterol, and slowing AS development. Importantly, our data also indicate that piperine works synergistically with established lipid-lowering medications, broadening its therapeutic potential. Despite the dose-dependent nature of piperine, its toxicity warrants careful attention. Future investigations will aim to clarify how piperine stimulates LXRα and to design novel piperine-based derivatives with reduced toxicity and enhanced cholesterol-excretion efficacy. Research will also consider the utility of BLEC or piperine in other lipid-related disorders, including non-alcoholic fatty liver disease. Collectively, these discoveries support a new therapeutic direction for enhancing cholesterol disposal in AS and lowering CVD risk, providing a scientific basis and new momentum for innovative drug development.

Acknowledgments: None

Conflict of Interest: None

Financial Support: None

Ethics Statement: None

References

1. Barquera S, Pedroza-Tobías A, Medina C, Hernández-Barrera L, Bibbins-Domingo K, Lozano R, et al. Global overview of the epidemiology of atherosclerotic cardiovascular disease. Arch Med Res. 2015;46:328–38. doi:10.1016/j.arcmed.2015.06.006
2. Houghton JL. Effect of cholesterol-lowering therapy on endothelial function. Circulation. 2001;104:E6. doi:10.1161/01.CIR.104.2.e6
3. Luo J, Yang H, Song B-L. Mechanisms and regulation of cholesterol homeostasis. Nat Rev Mol Cell Biol. 2020;21:225–45. doi:10.1038/s41580-019-0190-7
4. Collaboration CTT), Baigent C, Blackwell L, Cholesterol Treatment Trialists', et al. Efficacy and safety of more intensive lowering of LDL cholesterol: a meta-analysis of data from 170,000 participants in 26 randomised trials. Lancet. 376;2010:1670–81. doi:10.1016/S0140-6736(10)61350-5
5. Cannon CP, Blazing MA, Giugliano RP, McCagg A, White JA, Theroux P, et al. Ezetimibe added to statin therapy after acute coronary syndromes. N Engl J Med. 2015;372:2387–97. doi:10.1056/NEJMoa1410489
6. Sabatine MS, Giugliano RP, Keech AC, Honarpour N, Wiviott SD, Murphy SA, et al. Evolocumab and clinical outcomes in patients with cardiovascular disease. N Engl J Med. 2017;376:1713–22. doi:10.1056/NEJMoa1615664
7. Bowman L, Hopewell JC, Chen F, Wallendszus K, Stevens W. HPS3/TIMI55–REVEAL Collaborative Group. Effects of anacetrapib in patients with atherosclerotic vascular disease. N Engl J Med. 2017;377:1217–27.
8. Agarwal A, Mehta PM, Jacobson T, Shah NS, Ye J, Zhu J, et al. Fixed-dose combination therapy for the prevention of atherosclerotic cardiovascular disease. Nat Med. 2024;30:1199–209. doi:10.1038/s41591-024-02896-w
9. Berge KE, Tian H, Graf GA, Yu L, Grishin NV, Schultz J, et al. Accumulation of dietary cholesterol in sitosterolemia caused by mutations in adjacent ABC transporters. Science. 2000;290:1771–5. doi:10.1126/science.290.5497.1771
10. Repa JJ, Berge KE, Pomajzl C, Richardson JA, Hobbs H, Mangelsdorf DJ. Regulation of ATP-binding cassette sterol transporters ABCG5 and ABCG8 by the liver X receptors alpha and beta. J Biol Chem. 2002;277:18793–800. doi:10.1074/jbc.M109927200
11. Zelcer N, Tontonoz P. Liver X receptors as integrators of metabolic and inflammatory signaling. J Clin Invest. 2006;116:607–14. doi:10.1172/JCI27883

12. Wang B, Tontonoz P. Liver X receptors in lipid signalling and membrane homeostasis. Nat Rev Endocrinol. 2018;14:452–63. doi:10.1038/s41574-018-0037-x
13. Xu H, Zhang Y, Wang P, Zhang J, Chen H, Zhang L, et al. A comprehensive review of integrative pharmacology-based investigation: a paradigm shift in traditional Chinese medicine. Acta Pharmaceutica Sinica B. 2021;11:1379–99. doi:10.1016/j.apsb.2021.03.024
14. Hao P, Jiang F, Cheng J, Ma L, Zhang Y, Zhao Y. Traditional Chinese medicine for cardiovascular disease: evidence and potential mechanisms. J Am Coll Cardiol. 2017;69:2952–66. doi:10.1016/j.jacc.2017.04.041
15. Li S, Zhao Z, Null A, Li M. Mongolian medicine: from traditional practice to scientific development. Pharmacol Res. 2023;197:106977. doi:10.1016/j.phrs.2023.106977
16. Xing J. The clinical observation about Baolier Capsule treatment for hyperlipidemia. Chin J Tradit Med. 2005;2:1–2.
17. Pan X, Shi Y, Zhan H. Clinical observation of Baolier Capsule combined with western medicine in the treatment of hyperlipidemia. New Chin Med. 2015;47(6):4–5.
18. Gang H, Feng H, Huai S. Study on the hypolipidemic effect of Mongolian medicine Baolier capsules. Chin J Tradit Med. 2017;23:10.
19. Wei M, Li F, Guo K, Yang T. Exploring the active compounds of traditional Mongolian medicine baolier capsule (BLEC) in patients with coronary artery disease (CAD) based on network pharmacology analysis, molecular docking and experimental validation. Drug Des Devel Ther. 2023;17:459–76. doi:10.2147/DDDT.S395207
20. Zou R, Zhou Y, Lu Y, Zhao Y, Zhang N, Liu J. Preparation, pungency and bioactivity transduction of piperine from black pepper (piper nigrum L.): a comprehensive review. Food Chem. 2024;456:139980. doi:10.1016/j.foodchem.2024.139980
21. Patel SS, Acharya A, Ray RS, Agrawal R, Raghuwanshi R, Jain P. Cellular and molecular mechanisms of curcumin in prevention and treatment of disease. Crit Rev Food Sci Nutr. 2020;60:887–939. doi:10.1080/10408398.2018.1552244
22. Octavia MD, Hasmiwati H, Revilla G, Zaini E. Effect of multicomponent crystal of piperine-nicotinic acid on antihyperlipidemic activity in rats. Pak J Pharm Sci. 2023;36:1777–81.
23. Wei M, Li P, Guo K. The impact of PSRC1 overexpression on gene and transcript expression profiling in the livers of ApoE−/− mice fed a high-fat diet. Mol Cell Biochem. 2020;465:125–39. doi:10.1007/s11010-019-03673-x
24. Redinger RN. Nuclear receptors in cholesterol catabolism: molecular biology of the enterohepatic circulation of bile salts and its role in cholesterol homeostasis. J Lab Clin Med. 2003;142:7–20. doi:10.1016/S0022-2143(03)00088-X
25. Brown E, Heerspink HJ, Cuthbertson DJ, Wilding JP. SGLT2 inhibitors and GLP-1 receptor agonists: established and emerging indications. Lancet. 2021;398:262–76. doi:10.1016/S0140-6736(21)00536-5
26. Rina B. A brief discussion on the hematological system in traditional Mongolian and western medicine. Chin J Tradit Med. 2019;25(10):55–6.
27. Zhao C, Li S, Zhang J, Huang Y, Zhang L, Zhao F, et al. Current state and future perspective of cardiovascular medicines derived from natural products. Pharmacol Ther. 2020;216:107698. doi:10.1016/j.pharmthera.2020.107698
28. Hosseini H, Bagherniya M, Sahebkar A, Iraj B, Majeed M, Askari G, et al. The effect of curcumin-piperine supplementation on lipid profile, glycemic index, inflammation, and blood pressure in patients with type 2 diabetes mellitus and hypertriglyceridemia. Phytother Res. 2024;38:5150–61. doi:10.1002/ptr.8304
29. Wei M, LYu P, Li P, Hu J, Wu R, Ouyang Q, et al. Piperine's anti-atherosclerotic activity and mechanism of action in ApoE−/− mice. Chinese Pharmacol Bull. 2021;37(12):1659–65.
30. Wang L, Palme V, Rotter S, Schilcher N, Cukaj M, Wang D, et al. Piperine inhibits ABCA1 degradation and promotes cholesterol efflux from THP-1-derived macrophages. Mol Nutr Food Res. 2017;61(4):1500960. doi:10.1002/mnfr.201500960
31. Thomas AB, Choudhary DC, Raje A, Nagrik SS. Pharmacokinetics and pharmacodynamic herb-drug interaction of piperine with atorvastatin in rats. J Chromatogr Sci. 2021;59(4):371–80. doi:10.1093/chromsci/bmaa126

32. Lim ES, Lee SE, Park MJ, Han DH, Lee HB, Ryu B, et al. Piperine improves the quality of porcine oocytes by reducing oxidative stress. Free Radic Biol Med. 2024;213:1–10. doi:10.1016/j.freeradbiomed.2023.12.042
33. Huang W, Zhang J, Jin W, Yang J, Yu G, Shi H, et al. Piperine alleviates acute pancreatitis: a possible role for FAM134B and CCPG1 dependent ER-phagy. Phytomedicine. 2022;105:154361. doi:10.1016/j.phymed.2022.154361
34. Rafael Quijia C, Chorilli M. Characteristics, biological properties and analytical methods of piperine: a review. Crit Rev Anal Chem. 2020;50(1):62–77. doi:10.1080/10408347.2019.1573656
35. Srivastava S, Dewangan J, Mishra S, Divakar A, Chaturvedi S, Wahajuddin M, et al. Piperine and Celecoxib synergistically inhibit colon cancer cell proliferation via modulating Wnt/β-catenin signaling pathway. Phytomedicine. 2021;84:153484. doi:10.1016/j.phymed.2021.153484
36. Rahimi-Dehkordi N, Heidari-Soureshjani S, Rostamian S. A systematic review of the anti-seizure and antiepileptic effects and mechanisms of piperine. Cent Nerv Syst Agents Med Chem. 2024;24. doi:10.2174/0118715249297934240630111059
37. Han J, Zhang S, He J, Li T. Piperine: chemistry and biology. Toxins. 2023;15(12):696. doi:10.3390/toxins15120696
38. Takooree H, Aumeeruddy MZ, Rengasamy KR, Venugopala KN, Jeewon R, Zengin G, et al. A systematic review on black pepper (Piper nigrum L.): from folk uses to pharmacological applications. Crit Rev Food Sci Nutr. 2019;59(sup1):S210–43. doi:10.1080/10408398.2019.1565489
39. Balesaria S, Pattni SS, Johnston IM, Nolan JD, Appleby RN, Walters JR. Common genetic variants in the bile acid synthesis enzyme CYP7A1 are associated with severe primary bile acid diarrhea. Gastroenterology. 2022;163(2):517–9. doi:10.1053/j.gastro.2022.05.005